

Effect of helical angle on the performance of Savonius wind turbine

*Jae-Hoon Lee¹⁾, Young-Tae Lee²⁾ and Hee-Chang Lim³⁾

^{1, 2, 3)} *School of Mechanical Engineering, Pusan National University, Busan 609-735, Korea*

³⁾ *hclim@pusan.ac.kr*

ABSTRACT

This study is aiming to optimize the performance of helical Savonius wind turbine at varying twist angles. The power coefficient at different tip speed ratio(TSR) and torque coefficient at different azimuths when helical angle of blade is 0°, 45°, 90° and 135° were investigated in a condition that projection area and aspect ratio are consistently maintained. The flow characteristics were examined at every 1° from 0° to 360°. In a result, the highest maximum power coefficient occurred at helical angle of 45°. From the comparison of power coefficient with the varying azimuths, it is indicated that the difference between maximum and minimum power coefficient at 90° and 135° was less than that at 0° and 45°. Regarding the variation of torque coefficient at different shape models, as helical angle increases, the phase difference of torque coefficient became smaller.

1 Introduction

Due to excessive use of fossil energy, the world has faced serious problems such as energy depletion and environment pollution as its additional consequence. To overcome these problems, lots of alternatives to fossil fuels have been proposed. Among them, new renewable energy has drawn noticeable attention because of the significant amount of money invested into research and development fields by government and the diverse policies established by government in order to support to spread it to non-public field. According to the report published by Renewable Energy Policy Network for the 21st century (REN21) released in 2013, the amount of energy generated using new renewable energy has increased year by year. In 2012, the amount has grown by about 19% from the previous year. In particular, in case of wind energy, the additional capacity has much more increased rather than others among new renewable energies. The annual average growth rate of wind power capacity accumulated from 2007 and 2012 was reported to be about 25%.

Vertical Axis Wind Turbine (VAWT) can be divided into two groups; Darrieus and Savonius type. Darrieus turbine is a device that uses lift force generated by airfoil, whereas Savonius turbine exploits drag force. Savonius wind turbine invented in 1929, in particular, has an inherently simple shape compared to other types of wind turbines,

¹⁾ Graduate Student

²⁾ Graduate Student

³⁾ Professor

so that the cost to develop the device can be less expensive. Furthermore, it produces less noise and maintains stable performance in relatively low wind speed.

Recently, some researchers have been conducting researches on an optimization about VAWT based on an involvement in the field of experiments and numerical analysis. Akwa (2012) studied numerically the influence of overlap ratio of Savonius wind rotor. The results showed that maximum performance appears at overlap ratio equals to 0.15. Kamoji (2008) examined the influence of the aspect ratio between diameter and height of Savonius wind rotor and the increase of the number of stages on the performance. They also analysed how the performance of Savonius wind rotor changes when helical angle is 90°. And performance of low aspect ratio (0.88) was better than aspect ratio 0.93, 1.17, respectively. Saha (2006) reported the performance of a wind turbine with the twist blades in the wind tunnel. The result showed that the large twist angle had better performance in lower speed, but in the large twist angle, the negative torque was observed.

As seen these reviews, it is evident that many studies have been focusing on VAWTs. However, taking a close look at the design parameters worked on by those studies, one can recognize that there is lack of clear analysis as to how performance is affected as helical angle changes. Therefore, the main objective of this paper is to investigate the variation of power coefficient and the flow patterns of wind turbine at different helical angles based on a constant projection area which is an area of the wind rotor actually receiving the wind.

2 NUMERICAL ANALYSIS

2.1 Theoretical Background

It is difficult to evaluate the performance of wind rotor with different shapes. Because of that, it is important to express the performance using non-dimensional performance coefficient which has generality. The coefficients used for evaluating the performance of wind rotor are as follows: C_p (Power coefficient), C_T (Torque coefficient) and TSR (tip speed ratio). TSR is a coefficient used for presenting the wind rotor performance. TSR (Tip Speed Ratio) is defined as the ratio of the blade tip linear speed to the wind speed. TSR, denoted by λ , can be expressed as equation (1), where R denotes the rotor radius[m], n is revolution per minute (RPM) and V_∞ means free stream wind speed[m/s].

$$\lambda = \frac{\omega R}{V_\infty} = \frac{2\pi R n}{V_\infty} \quad (1)$$

The power coefficient, denoted by C_p , is a ratio of the power produced by the wind rotor to the power available at a specific wind speed. The power coefficient can be calculated by equation (2), where T is a torque[N · m], ρ denotes the air density[kg/m³] and A is an area covered by the rotor[m²].

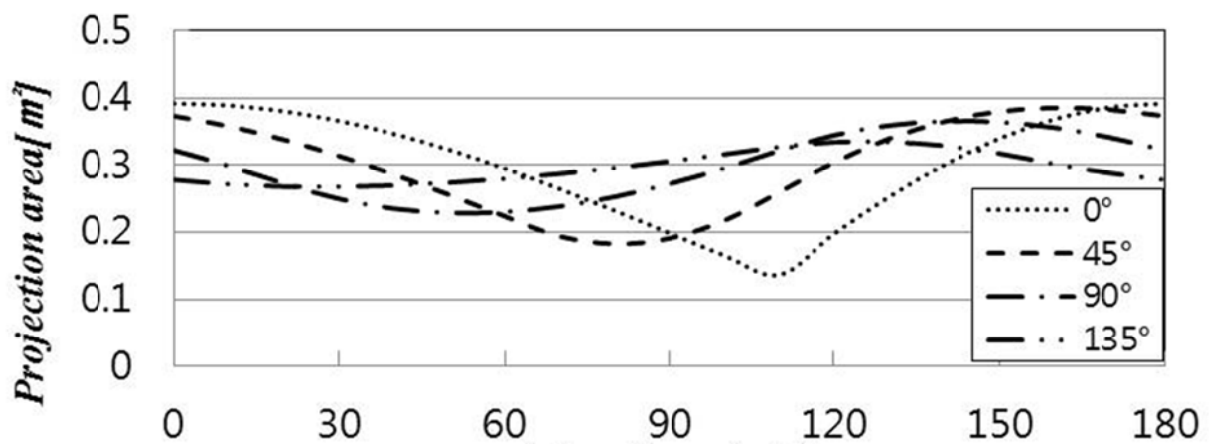
$$C_p = \frac{T\omega}{0.5\rho A V_\infty^3} \quad (2)$$

The torque coefficient, denoted by C_T , can be calculated by the equation (3). In case of a wind rotor using lift as propelling factor, the torque is generated using moment due to the lift produced by the rotating plane of the blade. On the other hand, in case of a drag-type wind rotor, the torque is generated using moment due to the drag.

$$C_T = \frac{T}{0.5\rho ARV_\infty^2} \quad (3)$$

2.2 shape of blades

In case of Savonius wind rotor, the projection area would change while blades rotate. Therefore, when the performance evaluation is carried out, this characteristic needs to be considered. In this study, variations of the projection area at different helical angles were taken into consideration. Even at different helical angle, the wind turbine has been designed to have all the identical average size of the projection area. Maximum, minimum and average projection areas are shown in Table 1 and Fig. 2. In this Table 1 and Fig.2 indicates that the difference between maximum and minimum projection area becomes smaller as helical angle grows bigger.



Helical angle	Minimum projection area [m ²]	Maximum projection area [m ²]	Average projection area [m ²]
0°	0.296m ²	0.392m ²	0.136m ²
45°	0.297m ²	0.386m ²	0.183m ²
90°	0.297m ²	0.366m ²	0.229m ²
135°	0.297m ²	0.335m ²	0.268m ²

3. Numerical Analysis

In this paper, the numerical analysis was also conducted using Fluent® which is one of commercial CFD (computational Fluid Dynamics) programs. Fluent is an analysis program utilizing finite volume method (FVM) based on the Navier-Stokes and energy equation, which is suited for resolving ambient flow and heat transfer problems for complicated shapes. Numerical domain and meshes were generated using Ansys ICEM. The number of meshes was distributed ranging from 1,200,000 to 1,500,000. For achieving fast calculation, the number of calculation repetitions was set to 50. In addition, the data has been stored after the flow was stabilized, e.g., around 5 rotation of the blade rotor. In terms of a turbulence model, In order to translate the operations of pressure and velocity, SIMPLE algorithm was used.

3.1 Governing Equation

A turbulence model employed in this paper requires analyzing URANS (Unsteady Reynolds Average Navier-Stokes). In this case, governing equations under Newton fluid condition requires two equations: continuous equation as expressed in Eq.(4) and momentum equation as expressed in Eq.(5). Considering the quality of the complicated turbulence and the swirling flow behind the rotating blade, the k-ε RNG turbulence model has been chosen.

Turbulence kinetic energy (k) for flow analysis is presented as equation (6). Turbulence kinetic energy dissipation rate (ε) is as equation (7). In these equations, C_μ , C_1 and C_2 are constants, which has the values of $C_\mu=0.0845$, $C_1=1.42$, and $C_2=1.68$, $C_\mu = 0.0845$, respectively.

$$\rho \frac{\partial u_i}{\partial x_j} = 0 \quad (4)$$

$$\rho \frac{Du_j}{Dt} = \rho \frac{\partial \tau_i}{\partial x_i} + \rho P_j \quad (5)$$

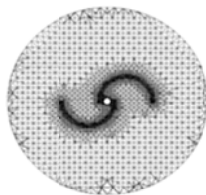
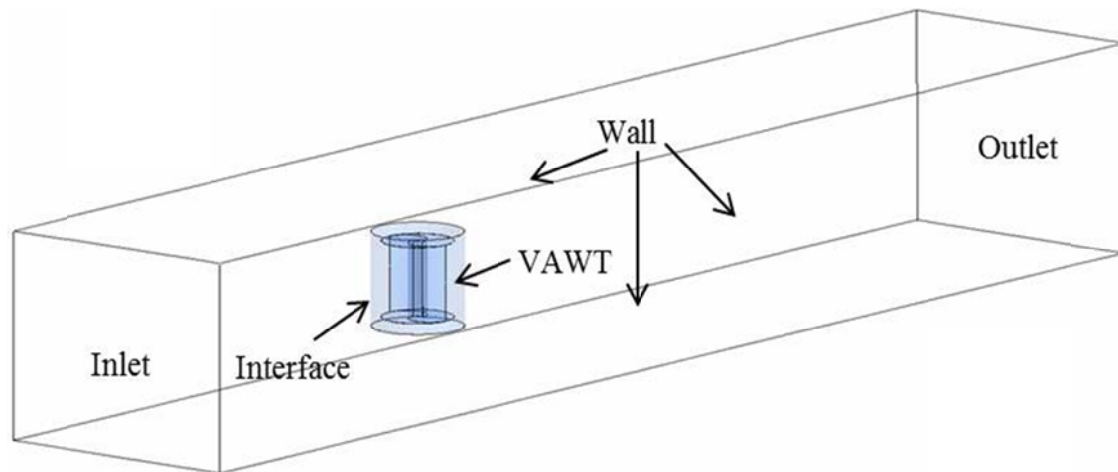
$$\rho \frac{Dk}{Dt} = \frac{\partial}{\partial x_j} \left(a_k \mu_{eff} \frac{\partial k}{\partial x_j} \right) + G_k + G_b - \rho \varepsilon - Y_M + S_k \quad (6)$$

$$\rho \frac{D\varepsilon}{Dt} = \frac{\partial}{\partial x_j} \left(a_\varepsilon \mu_{eff} \frac{\partial \varepsilon}{\partial x_j} \right) + C_{1\varepsilon} \frac{\varepsilon}{k} (G_k + G_{3\varepsilon} G_b) - C_{2\varepsilon} \rho \frac{\varepsilon^2}{k} - R_\varepsilon + S_\varepsilon \quad (7)$$

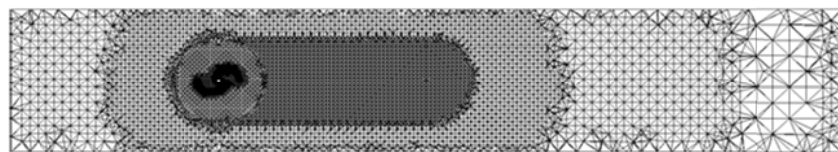
3.2 Boundary Conditions

For the appropriate analysis, the overall domain is divided into two sub-domain – surrounding fixed and inner rotating bladed domains. Total number of grid was 100~150million and grid shape was shown in Fig. 4. Fig. 4(a) and (b) are the main grid shape of rotating rotor and surrounding outer domain. In order to link the inner and outer domain, the interface condition is used for describe the detail of separated wake flow interacting the rotating and surrounding region. In general, the interface condition can be used for repetitive periodic or non-conformal calculation. In addition, the sliding mesh model(SMM) was used for (pseudo-)rotating mesh simulating the rotating blades. The sliding mesh can be effectively used in the case the mesh does not deform. The inlet condition was set to be 8m/s. In addition, the outlet condition in the domain was defined as a pressure outlet condition. Wall condition is applied to the side-, and

top/bottom wall planes. The moving wall condition was applied for all moving components such as the helical blades, main supporting pipe and end plates.



(a) Grid of shape of rotor



(b) Rotor and surrounding sub- domain

Fig. 4 Mesh and grid structure of VAWT

4. Results and discussion

To analyze the results, we compared power outputs with the varying TSR. In this study, the comparison between tunnel experiment and numerical calculation was all made. Based on the numerical analysis, torque coefficient was examined at varying azimuths in the condition where the blade is being rotated. Furthermore, it was also investigated that how air flow changes at different azimuths of Savonius wind turbine.

3.1 Comparison of power coefficient

Fig. 5 shows the power coefficients obtained in numerical study. it is noted that the maximum power coefficients are placed mostly in the range of TSR from 0.6 to 0.7 in both cases. The highest power coefficient appears at helical angle of 45°. At this angle, the highest power coefficient reaches around 0.2 when TSR equals to 0.55. At 90° and 135° of helical angle, the power coefficients look similar.

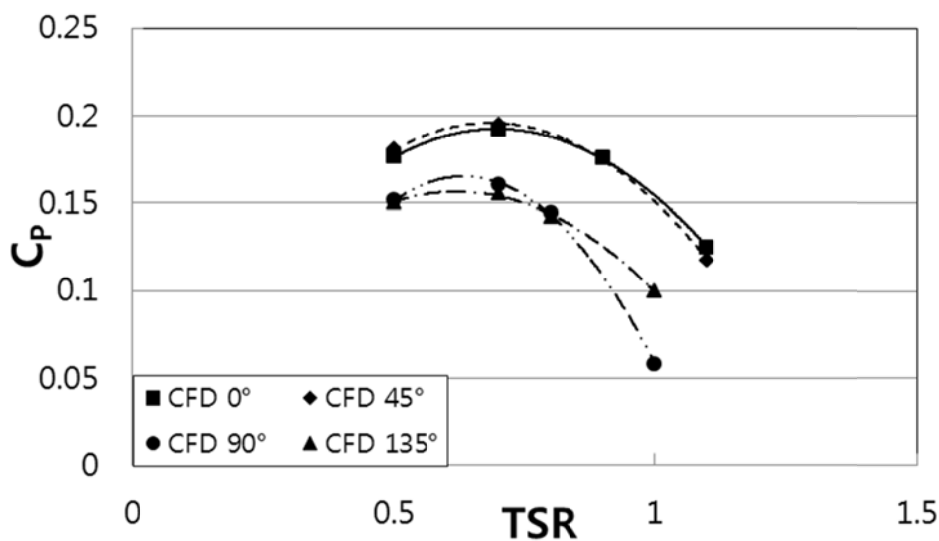


Fig. 5 Power coefficient variations against TSR

In order to correct the blockage effect in the wind tunnel test, the blockage ratio should be considered. The blockage ratio is defined as the ratio of wind tunnel cross sectional area(C) to the projected area of the rotor(S). As the blockage ratio increases, the power coefficient increases. When the blockage ratio is placed in between 1 and 30%, Alexander (1978) suggested a typical correction ration of velocity, as shown in fig.6. In the figure, V and V_c are the original and corrected velocity, respectively (e.g., $V=8\text{m/s}$, $V_c=9.36\text{m/s}$ in this study). After the correction is made, the overall power coefficient decreases about 37%. Therefore, when helical angle is 45° , the maximum power coefficient reach 0.12 at $\text{TSR} = 0.7$.

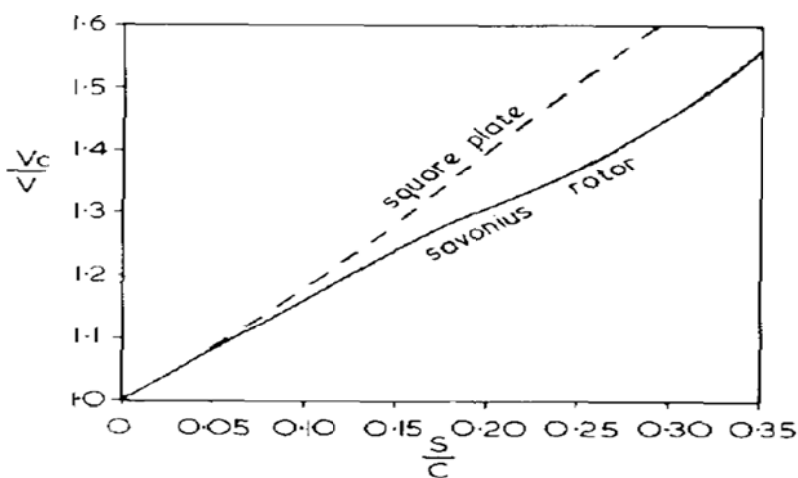
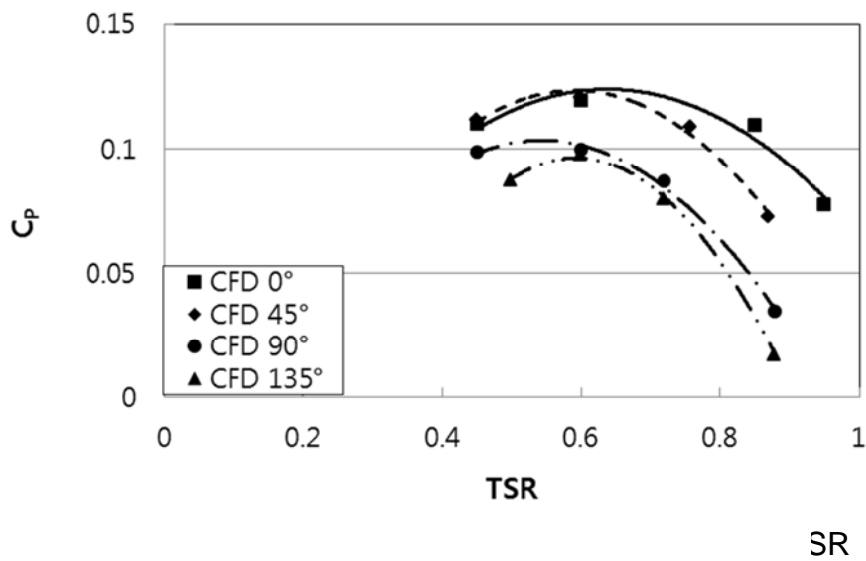


Fig. 6 Variation of velocity correction factor with S/C. (Alexander, 1978)



3.2 Temporal variation of torque coefficient at different azimuths

Fig. 8 shows torque coefficients at different azimuths. While horizontal axis represents azimuth, vertical axis represents torque coefficient. At varying azimuths, torque coefficient becomes highest to be 0.455, at helical angle of 45° and TSR of 0.4. The graphs also indicate that phase difference of torque coefficient gets lower, as helical angle increases. At helical angle of 135°, the phase difference becomes lowest. The reason seems that a difference between maximum and minimum projection areas is lowest. Negative torque coefficient occurs in the range of 80°-100° and 260°-280° at helical angle of 0°, 45° and TSR of 0.8, respectively. Regarding this observation, which we are going to explain later, it is inferred that a force by air is not be transferred to concave surfaces of both blades properly. Instead, the force might affect convex surfaces. However, in case that TSR is lower than 0.8, negative value does not occur. The reason seems that a force of air resistance gets greater at convex part of blade than rotation power of turbine, as spinning speed gets faster. However, the blades with helical angle of 90° and 135° do not show any negative value of torque coefficient at TSR=0.8.

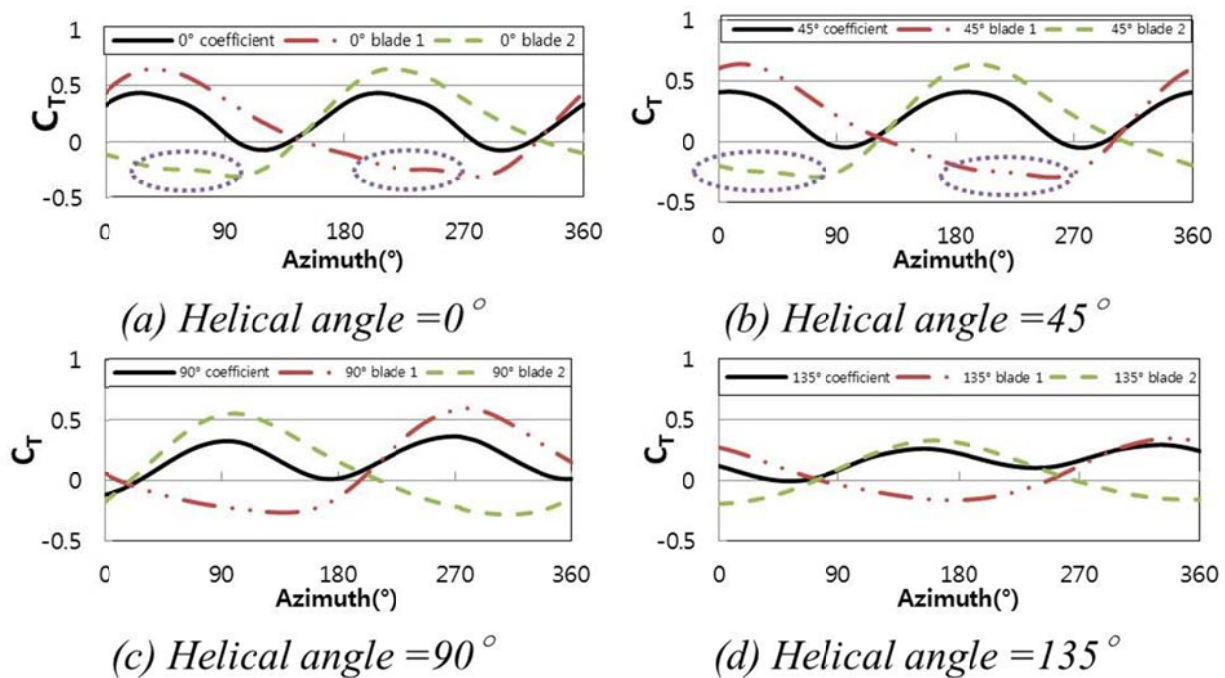


Fig. 8 Torque coefficient at different azimuth

4 Conclusion

This paper has investigated the performance characteristics of Savonius wind turbine at different helical angles through numerical analysis and performance evaluation conducted in large-scale boundary layer wind tunnel. The key conclusions are summarized as follows,

- 1) It is verified that the range of tip speed ratio (TSR) and maximum power coefficient change as Savonius wind turbine blade helical angle varies.
- 2) From experimental and numerical results, the highest power coefficient appears to be about 0.3 at helical angle of 45° . However, at helical angle of 90° and 135° , power coefficient becomes lower than that at 0° and their maximum power coefficients appear similar. The reason is inferred that convex surface of the blade is consistently affected by the air resistance when the helical angle grows bigger than a specific angle.
- 3) At helical angle of 0° and 45° , negative torque coefficient occurs when $TSR=0.8$. This is the only observation of negative torque coefficient. The reason is inferred that convex surface of the blade receives a fluid force more densely than at concave surface when azimuth is close to 90° .
- 4) At helical angle of 135° , torque coefficient values appear consistent. The reason is inferred that there is no difference in the size of the area where receives the force of air.
- 5) It is implied that output power could be maintained to be higher if the number of rotations is controlled to be TSR of 0.6 at helical angle of 45° .

Acknowledgements

This work was supported by the Human Resources Development of the Korea Institute of Energy Technology Evaluation and Planning (KETEP) grant funded by the Korea government Ministry of Knowledge Economy (No. 20114010203080).

References

- Renewable Energy Policy Network for the 21st century (2013), "Renewable 2013 Global status Report".
- Akwa, J.V., da Silva Júnior, G.A., Petry, A.P. (2012), "Discussion on the verification of the overlap ratio influence on performance coefficients of a Savonius wind rotor using computational fluid dynamics", *Renewable Energy*, **38**, 141-149.
- Kamoji, M.A., Kedare, S.B., Prabhu, S.V. (2008), "Experimental investigations on single stage, two stage and three stage conventional Savonius rotor", *Int. J. Energy Res.*, **32**, 877-895.
- Kamoji, M.A., Kedare, S.B., Prabhu, S.V. (2009), "Performance tests on helical Savonius rotors", *Renewable Energy*, **34**, 521-529.
- Saha, U. K., Rajkumar, M. J. (2006), " On the performance analysis of Savonius rotor with twisted blades", *Renewable Energy*, **31**, 1776-1788.
- Mohamed, M.H., Janiga, G., Pap, E., Théevenin, D. (2010), "Optimization of Savonius turbines using an obstacle shielding the returning blade", *Renewable Energy*, **35**, 2618-2626.
- Fujisawa, N. (1992), "On the torque mechanism of Savonius rotors", *Journal of Wind Engineering and Industrial Aerodynamics*, **40**, 27-292.
- Alexander, A.J. , Holownia, B.P. (1978), "Wind tunnel test on a savonius rotor", *Journal of Wind Engineering and Industrial Aerodynamics*, **3**(4), 343-351.